Supplementary Information

Near Sunlight Continuous Broadband White-Light Emission by Single-Phase Zn(II)-1,3,5-benzenetricarboxylate MOFs

Ce Wang, Zheng Yin*, Wei-Min Ma, Xi-Yao Li, Li-Hui Cao, Yu Cheng, Xin-Yu Yu and Yang-Min Ma*

College of Chemistry and Chemical Engineering, Shaanxi Key Laboratory of Chemical Additives for Industry, Shaanxi University of Science and Technology, Xi'an 710021, P. R. China.

Email: yinzheng@sust.edu.cn

Materials and physical measurements

The metal salt and the organic ligand of H_3btc, H_2gac used in the MOFs synthesis were purchased from Aladdin Co. All the organic solvents were purchased from Xilong Scientific Co. The materials are used without further purification unless otherwise specified. The anhydrous dichloromethane and acetonitrile for solvent exchange were purchased from Aladdin Co.

The powder X-ray diffraction (PXRD) intensities were measured at 298 K on a Rigaku D/max-IIIA diffractometer (Cu-K_α, λ = 1.54056 Å). The sample was prepared by crushing the MOFs crystals into powder and then scanned from 3 to 60° at a rate of 5 °/min. Calculated PXRD patterns of **1** were generated using Materials Studio (4.0) program. The IR spectrum was recorded in a Bruker TENSOR-II FTIR Spectrometer. The thermogravimetric analyses (TGA) were performed on a TGA-55 instrument in flowing N_2 under a heating rate of 5 °C/min. Both the fluorescence spectrums of **1** in solid state and in solution were measured in a Edinburgh FL-980 spectrophotometer.

Synthesis of $\{[NH_2(CH_3)_2]_6[Zn_{16}(btc)_{12}(gac)(DMA)_3(H_2O)_3]\}\cdot 17DMA$ (1)

(i) Traditional solvothermal synthesis. A DMA solution (15 mL) containing $Zn(NO_3)_2\cdot 6H_2O$ (0.2 mmol, 59.7 mg), H_3btc (0.2 mmol, 42.1 mg) and H_2gac (0.4 mmol, 30.0mg) in a Teflon-lined steel bomb was heated at 140 °C for 72 h. The autoclave was cooled at a rate of 10 °C h^{-1} to room temperature. Colorless block crystals of **1** were collected, washed with DMA, and dried in air with yield of 84.6% based on Zn. Elemental analysis (%) Calcd. for $C_{202}H_{273}N_{26}Zn_{16}O_{98}$: H, 4.84; C, 42.71; N, 6.41. Found: H, 4.59; C, 43.10; N, 6.23. IR data for **1** (KBr, cm^{-1}): 3443(s), 2930(w), 1638(s), 1560(w), 1481(s), 1463(s), 1322(m), 1221(s), 1120(s), 1092(s), 967(w), 865(s), 746(m), 625(w), 485(w). The glycolic acid (H_2gac) is excessive than H_3btc with proportion of 2:1 in the starting reaction solution, while the ratio of H_2gac to H_3btc in the MOFs is just 1:12. The contrast experiment without glycolic acid showed no formation of the presented MOFs, but a known Cd(II)-btc MOFs of $[Zn_2(btc)(NO_3)(DMA)_3]$ with CCDC number of 838769.[5] Hence, the H_2gac was an auxiliary multidentate and bridging ligand, which direct the construction of the MOFs with unprecedented sophistication in crystallographic asymmetric unit.

(ii) Microwave-assisted solvothermal synthesis. The same reaction solution of the traditional solvothermal method was placed in a 60 mL Teflon-lined autoclave, which was then inserted into the cavity of a microwave reactor. The reaction mixture was maintained at 140 °C, 300W, and 6.3 atm for a total of 30 min. After the reaction solution has been cooled to room temperature (ca. 2 h), the colorless crystals of **1** were collected by filtration, washed with DMA, and dried in air, giving a yield of 70.8% based on Zn.

Single crystal X-ray diffraction analyses

The single-crystal diffraction data of **1** were collected on a Rigaku XtaLAB Synergy four-circle diffractometer under Cu-*K*α radiation (λ = 1.54056 Å), with the CrysAlisPro software (version 1.171.39.34b) for data reduction and analysis. The structure was solved by direct methods and refined by full-matrix least-squares method on F^2 using SHELX algorithms in Olex2.[1, 2] All non-hydrogen atoms were refined with anisotropic displacement parameters. All hydrogen atoms were generated geometrically. The disordered guest molecules which cannot be modeled were treated by the SQUEEZE routine.[3, 4] The contributions of 3649 electrons per unit-cell, ie 912 electrons per formula unit were removed. The removed materials during SQUEEZE process are 3 counter cations of $[H_2N(CH_3)_2]^+$ and 16 DMA guest molecules per formula (Cal. 849 electrons in total), which are defined by considering charge balance, thermogravimetry and elemental analysis results. The structure figures were produced by Diamond 4.0 software.

The sample of **1** processes good shape and transparency for single crystal diffraction. However, the collected data exhibits high wR_2 value of 0.53 after several attempts with optimized measurement parameters. The possible reasons may stem from the unusual sophistication of crystallographic asymmetric unit with sixteen metal ions and twelve ligands. In addition, due to disorder of the coordinated DMA and H_2O, as well as guest solvent, command including DFIX, FLAT and IOSR were used to restrain the solvent molecules. Given that the high structure complexity with several heavy-atoms of **1**, it was not possible to see clear electron-density peaks in difference maps which would correspond with acceptable locations for the H atoms bonded to water oxygen atoms, the refinement was completed with no allowance for these H atoms in the model.

The CCDC reference numbers are 1943080 for **1**. The supplementary crystallographic data for **1** can be found in the Supporting Information or can be obtained free of charge from the Cambridge Crystallographic Data Centre via http://www.ccdc.cam.ac.uk/data_request/cif. Crystallographic details are provided in Table S1, and the selected bond lengths and angles are listed in Table S2-3.

Table S1 Crystal data and structure refinement for **1**.

Empirical formula	$C_{202}H_{273}N_{26}Zn_{16}O_{98}$
Formula weight	5679.99
Temperature / K	100
Radiation / Å	1.54184 (Cu $K\alpha$)
Crystal system	Monoclinic
Space group	$P2_1/c$
a / Å	35.8753 (3)
b / Å	24.4464 (2)
c / Å	32.1563 (3)
α / °	90
β / °	114.077 (1)
γ / °	90
V / Å^3	25748.2 (4)
Z	4
$F(000)$	8492
D_c./ g cm^{-3}	1.090
μ / mm^{-1}	2.17
Reflns. coll.	150740
Unique reflns.	51918
R_{int}	0.029
$^aR_1$ [I⩾2σ(I)]	0.136
$^bwR_2$ (all data)	0.533
GOF	1.04
Void	55.8%
CCDC number	1943080

$^aR_1 = \Sigma||F_o| - |F_c||/\Sigma|F_o|$. $^bwR_2 = [\Sigma w(F_o^2 - F_c^2)^2/\Sigma w(F_o^2)^2]^{1/2}$.

Table S2 The selected bond lengths of **1**.

Zn1—O23^{ii}	2.052 (5)	Zn9—O40^{ix}	1.938 (5)
Zn1—O24^{iii}	2.090 (5)	Zn9—O50^{x}	1.975 (5)
Zn1—O63	2.028 (5)	Zn9—O57^{ix}	1.947 (6)
Zn1—O64^{i}	2.025 (5)	Zn9—O67	1.907 (5)
Zn1—O260^{iii}	1.980 (6)	Zn10—O28	1.920 (6)
Zn2—O4^{ii}	1.989 (7)	Zn10—O35	1.934 (8)
Zn2—O41^{iv}	1.967 (8)	Zn10—O37	1.957 (6)
Zn2—O42^{iv}	2.440 (10)	Zn10—O44^{iii}	1.943 (6)
Zn2—O65	1.971 (7)	Zn11—O9	1.966 (5)
Zn2—O77	1.920 (6)	Zn11—O17	1.942 (5)
Zn3—O11^{v}	1.982 (6)	Zn11—O19	1.999 (5)
Zn3—O45	1.951 (6)	Zn11—O25	1.935 (6)
Zn3—O61	1.976 (7)	Zn12—O10	1.942 (6)
Zn3—O80	1.923 (15)	Zn12—O13^{xi}	2.415 (10)
Zn4—O12^{v}	1.990 (7)	Zn12—O14^{xi}	1.969 (6)
Zn4—O46	1.883 (10)	Zn12—O20	1.975 (6)
Zn4—O55	1.911 (6)	Zn12—O26	1.941 (6)
Zn4—O62	1.949 (6)	Zn13—O15^{xi}	2.030 (5)
Zn5—O47	1.958 (6)	Zn13—O16^{vi}	1.987 (5)
Zn5—O51	1.950 (5)	Zn13—O21	1.957 (5)
Zn5—O69^{iv}	1.935 (5)	Zn13—O31^{vi}	2.351 (9)
Zn5—O70^{vi}	2.000 (4)	Zn13—O32^{vi}	2.072 (6)
Zn6—O36^{iii}	1.993 (9)	Zn14—O5	1.968 (6)
Zn6—O38^{iii}	2.031 (7)	Zn14—O7	1.928 (6)
Zn6—O43	2.025 (8)	Zn14—O33^{xii}	2.140 (7)
Zn6—O73	2.005 (7)	Zn14—O34^{xii}	2.260 (6)
Zn6—O79	2.105 (10)	Zn14—O60^{xiii}	1.977 (6)
Zn7—O6^{vii}	2.054 (6)	Zn14—C53^{xii}	2.510 (9)
Zn7—O34^{iii}	2.158 (6)	Zn15—O3	1.944 (6)
Zn7—O59^{vi}	2.032 (6)	Zn15—O29^{xiv}	1.932 (6)
Zn7—O74	2.163 (9)	Zn15—O66^{xv}	1.994 (9)

Zn7—O75	2.164 (8)	Zn15—O81	1.961 (11)
Zn7—O76	2.091 (7)	Zn16—O1	2.026 (5)
Zn8—O39	1.925 (6)	Zn16—O2^{xvi}	2.040 (5)
Zn8—O49^{viii}	1.993 (5)	Zn16—O53^{xiii}	2.060 (5)
Zn8—O58	1.943 (5)	Zn16—O54^{xiv}	2.079 (4)
Zn8—O71	1.928 (5)	Zn16—O78	1.970 (5)

Symmetry codes: (i) -*x*+3, -*y*+1, -*z*+2; (ii) *x*+1, *y*, *z*+1; (iii) -*x*+2, -*y*+1, -*z*+1; (iv) -*x*+2, *y*-1/2, -*z*+3/2; (v) *x*+1, -*y*+3/2, *z*+1/2; (vi) *x*, -*y*+3/2, *z*-1/2; (vii) *x*+1, *y*, *z*; (viii) *x*, -*y*+3/2, *z*+1/2; (ix) -*x*+2, *y*+1/2, -*z*+3/2; (x) -*x*+2, -*y*+2, -*z*+1; (xi) -*x*+1, *y*+1/2, -*z*+1/2; (xii) -*x*+1, -*y*+1, -*z*+1; (xiii) *x*-1, -*y*+3/2, *z*-1/2; (xiv) -*x*+1, *y*-1/2, -*z*+1/2; (xv) *x*-1, *y*, *z*-1; (xvi) -*x*, -*y*+1, -*z*; (xvii) *x*-1, *y*, *z*.

Table S3 The selected bond angles of **1**.

O23^{ii}—Zn1—O24^{iii}	159.4 (2)	O40^{ix}—Zn9—O50^{x}	107.6 (2)
O63—Zn1—O23^{ii}	89.0 (2)	O40^{ix}—Zn9—O57^{ix}	125.8 (3)
O63—Zn1—O24^{iii}	87.0 (2)	O57^{ix}—Zn9—O50^{x}	105.0 (3)
O64^{i}—Zn1—O23^{ii}	89.0 (2)	O67—Zn9—O40^{ix}	105.6 (3)
O64^{i}—Zn1—O24^{iii}	87.1 (2)	O67—Zn9—O50^{x}	108.4 (2)
O64^{i}—Zn1—O63	157.6 (2)	O67—Zn9—O57^{ix}	103.7 (2)
O260^{iii}—Zn1—O23^{ii}	101.3 (3)	O28—Zn10—O35	107.4 (3)
O260^{iii}—Zn1—O24^{iii}	99.3 (3)	O28—Zn10—O37	97.0 (3)
O260^{iii}—Zn1—O63	98.6 (2)	O28—Zn10—O44^{iii}	112.0 (3)
O260^{iii}—Zn1—O64^{i}	103.7 (2)	O35—Zn10—O37	108.3 (3)
O4^{ii}—Zn2—O42^{iv}	134.9 (3)	O35—Zn10—O44^{iii}	115.7 (3)
O41^{iv}—Zn2—O4^{ii}	94.3 (3)	O44^{iii}—Zn10—O37	114.7 (3)
O41^{iv}—Zn2—O42^{iv}	56.4 (3)	O9—Zn11—O19	103.3 (2)
O41^{iv}—Zn2—O65	110.1 (4)	O17—Zn11—O9	101.9 (2)
O65—Zn2—O4^{ii}	121.3 (3)	O17—Zn11—O19	107.9 (2)
O65—Zn2—O42^{iv}	102.0 (3)	O25—Zn11—O9	128.5 (2)
O77—Zn2—O4^{ii}	92.8 (3)	O25—Zn11—O17	106.8 (3)
O77—Zn2—O41^{iv}	131.4 (4)	O25—Zn11—O19	107.2 (3)
O77—Zn2—O42^{iv}	85.9 (3)	O10—Zn12—O13^{xi}	94.8 (3)
O77—Zn2—O65	106.6 (3)	O10—Zn12—O14^{xi}	111.4 (3)
O45—Zn3—O11^{v}	106.8 (3)	O10—Zn12—O20	115.4 (3)
O45—Zn3—O61	122.5 (3)	O14^{xi}—Zn12—O13^{xi}	57.5 (3)
O61—Zn3—O11^{v}	97.5 (4)	O14^{xi}—Zn12—O20	89.2 (3)
O80—Zn3—O11^{v}	105.3 (5)	O20—Zn12—O13^{xi}	142.3 (3)
O80—Zn3—O45	117.8 (5)	O26—Zn12—O10	107.5 (4)
O80—Zn3—O61	104.0 (5)	O26—Zn12—O13^{xi}	87.2 (3)
O46—Zn4—O12^{v}	106.4 (4)	O26—Zn12—O14^{xi}	128.4 (4)
O46—Zn4—O55	111.2 (4)	O26—Zn12—O20	103.5 (3)
O46—Zn4—O62	119.0 (4)	O15^{xi}—Zn13—O31^{vi}	150.1 (2)
O55—Zn4—O12^{v}	94.9 (3)	O15^{xi}—Zn13—O32^{vi}	94.2 (2)
O55—Zn4—O62	115.0 (3)	O16^{vi}—Zn13—O15^{xi}	100.9 (2)

O62—Zn4—O12^{v}	107.1 (3)	O16^{vi}—Zn13—O31^{vi}	86.6 (3)
O47—Zn5—O70^{vi}	94.7 (2)	O16^{vi}—Zn13—O32^{vi}	123.1 (3)
O51—Zn5—O47	113.9 (2)	O21—Zn13—O15^{xi}	104.2 (2)
O51—Zn5—O70^{vi}	105.64 (18)	O21—Zn13—O16^{vi}	116.2 (2)
O69^{iv}—Zn5—O47	118.9 (3)	O21—Zn13—O31^{vi}	98.0 (3)
O69^{iv}—Zn5—O51	114.8 (2)	O21—Zn13—O32^{vi}	112.3 (2)
O69^{iv}—Zn5—O70^{vi}	105.4 (2)	O32^{vi}—Zn13—O31^{vi}	58.5 (3)
O36^{iii}—Zn6—O38^{iii}	99.2 (4)	O5—Zn14—O33^{xii}	104.3 (3)
O36^{iii}—Zn6—O43	107.7 (3)	O5—Zn14—O34^{xii}	101.5 (3)
O36^{iii}—Zn6—O73	127.8 (4)	O5—Zn14—O60^{xiii}	104.1 (3)
O36^{iii}—Zn6—O79	86.9 (6)	O7—Zn14—O5	109.1 (3)
O38^{iii}—Zn6—O79	173.5 (6)	O7—Zn14—O33^{xii}	100.6 (3)
O43—Zn6—O38^{iii}	92.1 (4)	O7—Zn14—O34^{xii}	147.1 (3)
O43—Zn6—O79	84.0 (5)	O7—Zn14—O60^{xiii}	93.6 (3)
O73—Zn6—O38^{iii}	87.5 (3)	O33^{xii}—Zn14—O34^{xii}	59.2 (2)
O73—Zn6—O43	123.9 (3)	O60^{xiii}—Zn14—O33^{xii}	141.8 (3)
O73—Zn6—O79	90.4 (5)	O60^{xiii}—Zn14—O34^{xii}	90.5 (2)
O6^{vii}—Zn7—O34^{iii}	103.0 (2)	O3—Zn15—O66^{xv}	120.7 (3)
O6^{vii}—Zn7—O74	161.6 (3)	O3—Zn15—O81	104.8 (4)
O6^{vii}—Zn7—O75	85.8 (3)	O29^{xiv}—Zn15—O3	113.3 (3)
O6^{vii}—Zn7—O76	89.6 (3)	O29^{xiv}—Zn15—O66^{xv}	95.1 (4)
O34^{iii}—Zn7—O74	94.9 (3)	O29^{xiv}—Zn15—O81	126.1 (4)
O34^{iii}—Zn7—O75	171.0 (3)	O81—Zn15—O66^{xv}	96.8 (5)
O59^{vi}—Zn7—O6^{vii}	91.3 (3)	O1—Zn16—O2^{xvi}	159.0 (2)
O59^{vi}—Zn7—O34^{iii}	88.5 (2)	O1—Zn16—O53^{xiii}	89.0 (2)
O59^{vi}—Zn7—O74	93.2 (3)	O1—Zn16—O54^{xiv}	87.5 (2)
O59^{vi}—Zn7—O75	93.3 (3)	O2^{xvi}—Zn16—O53^{xiii}	89.6 (2)
O59^{vi}—Zn7—O76	173.5 (3)	O2^{xvi}—Zn16—O54^{xiv}	86.3 (2)
O74—Zn7—O75	76.2 (3)	O53^{xiii}—Zn16—O54^{xiv}	158.7 (2)
O76—Zn7—O34^{iii}	85.0 (4)	O78—Zn16—O1	97.5 (2)
O76—Zn7—O74	87.9 (4)	O78—Zn16—O2^{xvi}	103.0 (2)
O76—Zn7—O75	93.2 (4)	O78—Zn16—O53^{xiii}	105.5 (2)

O39—Zn8—O49$^{\text{viii}}$	108.7 (3)	O78—Zn16—O54$^{\text{xiv}}$	95.7 (2)
O39—Zn8—O58	112.7 (3)		
O39—Zn8—O71	116.6 (3)		
O58—Zn8—O49$^{\text{viii}}$	109.1 (3)		
O71—Zn8—O49$^{\text{viii}}$	91.2 (2)		
O71—Zn8—O58	115.9 (3)		

Symmetry codes: (i) $-x+3, -y+1, -z+2$; (ii) $x+1, y, z+1$; (iii) $-x+2, -y+1, -z+1$; (iv) $-x+2, y-1/2, -z+3/2$; (v) $x+1, -y+3/2, z+1/2$; (vi) $x, -y+3/2, z-1/2$; (vii) $x+1, y, z$; (viii) $x, -y+3/2, z+1/2$; (ix) $-x+2, y+1/2, -z+3/2$; (x) $-x+2, -y+2, -z+1$; (xi) $-x+1, y+1/2, -z+1/2$; (xii) $-x+1, -y+1, -z+1$; (xiii) $x-1, -y+3/2, z-1/2$; (xiv) $-x+1, y-1/2, -z+1/2$; (xv) $x-1, y, z-1$; (xvi) $-x, -y+1, -z$; (xvii) $x-1, y, z$.

Table S4 The calculated Zn···Zn distance in the dinuclear [Zn2] unit of **1**.

Zn1—Zn1^{xxiv}	3.0025(0)	Zn7—Zn14^{xix}	3.4338(0)
Zn2—Zn15^{xvii}	3.8743(1)	Zn8—Zn9^{xx}	3.2925(0)
Zn3—Zn4	3.4128(0)	Zn11—Zn12	3.3062(0)
Zn5—Zn5^{xviii}	3.8882(0)	Zn13—Zn13^{xxii}	4.0280(0)
Zn6—Zn10^{xviii}	3.5449(0)	Zn16—Zn16^{xxiii}	2.9834(0)

Symmetry codes: (v) -*x*+3, 1-*y*, 3-*z*; (xvii) *x*-1, *y*, *z*; (xviii) -*x*+2, -*y*+1, -*z*+2; (xix) *x*-1, *y*, *z*; (xx) -*x*+2, *y*+1/2, -*z*+5/2; (xxii) -*x*+1, -*y*+2, -*z*+1; (xxiii) -*x*, -*y*+1, -*z*+1; ; (xxiv) -*x*+3, 1-*y*, 3-*z*.

Table S5 The calculated coordination geometry of each metal centre of **1** by Shape 4.0, based on the simaller Continuous Shape Measures (CShM) value. Coordination geometry: SPY-5 = Spherical square pyramid, vOC-5 = Vacant octahedron, T-4 = Tetrahedron, SS-4 = Seesaw, TBPY-5 = Trigonal bipyramid, OC-6 = Octahedron, TPR-6 = Trigonal prism. The preferred geometries with lower CShM values are highlighted in blue.

Metal ions	Coordination Numbers	Geometry	CShM value
Zn1	5	SPY-5	0.242
		vOC-5	0.836
Zn2	4	T-4	2.947
		SS-4	4.930
Zn3	4	T-4	0.709
		SS-4	6.507
Zn4	4	T-4	0.621
		SS-4	8.319
Zn5	4	T-4	0.738
		SS-4	7.565
Zn6	5	TBPY-5	0.573
		SPY-5	4.186
Zn7	6	OC-6	0.995
		TPR-6	12.341
Zn8	4	T-4	0.916
		Seesaw	8.408
Zn9	4	T-4	0.698
		Seesaw	5.640
Zn10	4	T-4	0.475
		Seesaw	8.434
Zn11	4	T-4	0.922
		Seesaw	5.108
Zn12	5	SPY-5	2.943
		vOC-5	5.386
Zn13	5	SPY-5	3.238
		TBPY-5	3.553
Zn14	5	SPY-5	1.750
		vOC-5	3.522
Zn15	4	T-4	1.978
		Seesaw-4	5.840
Zn16	5	SPY-5	0.339
		vOC-5	0.856

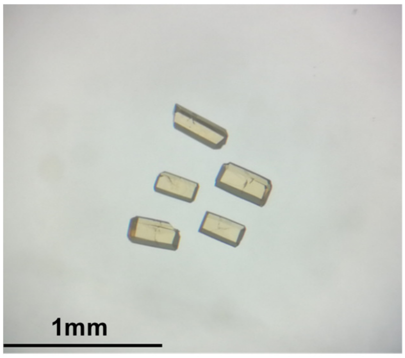

Figure S1 The photos of crystals of **1** synthesized under traditional solvothermal reaction.

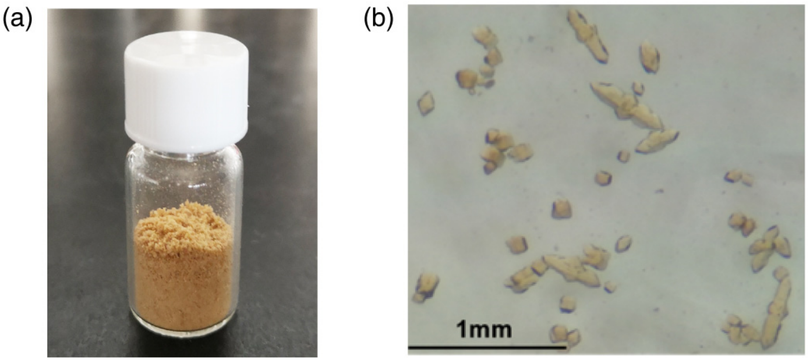

Figure S2 (a) The photo of crystals of **1** (0.96 g) synthesized by microwave-assisted solvothermal reaction on gram scale. The presented bottle of crystals were generated in 2.5 hours including 30 min thermal reaction and 2 hour cooling, using 12 microwave autoclaves. (b) The photo of crystals of **1** synthesized under microwave-assisted solvothermal synthesis, which shows high phase homogeneity comparing to the traditional solvothermal reaction excepting decresased crystal size.

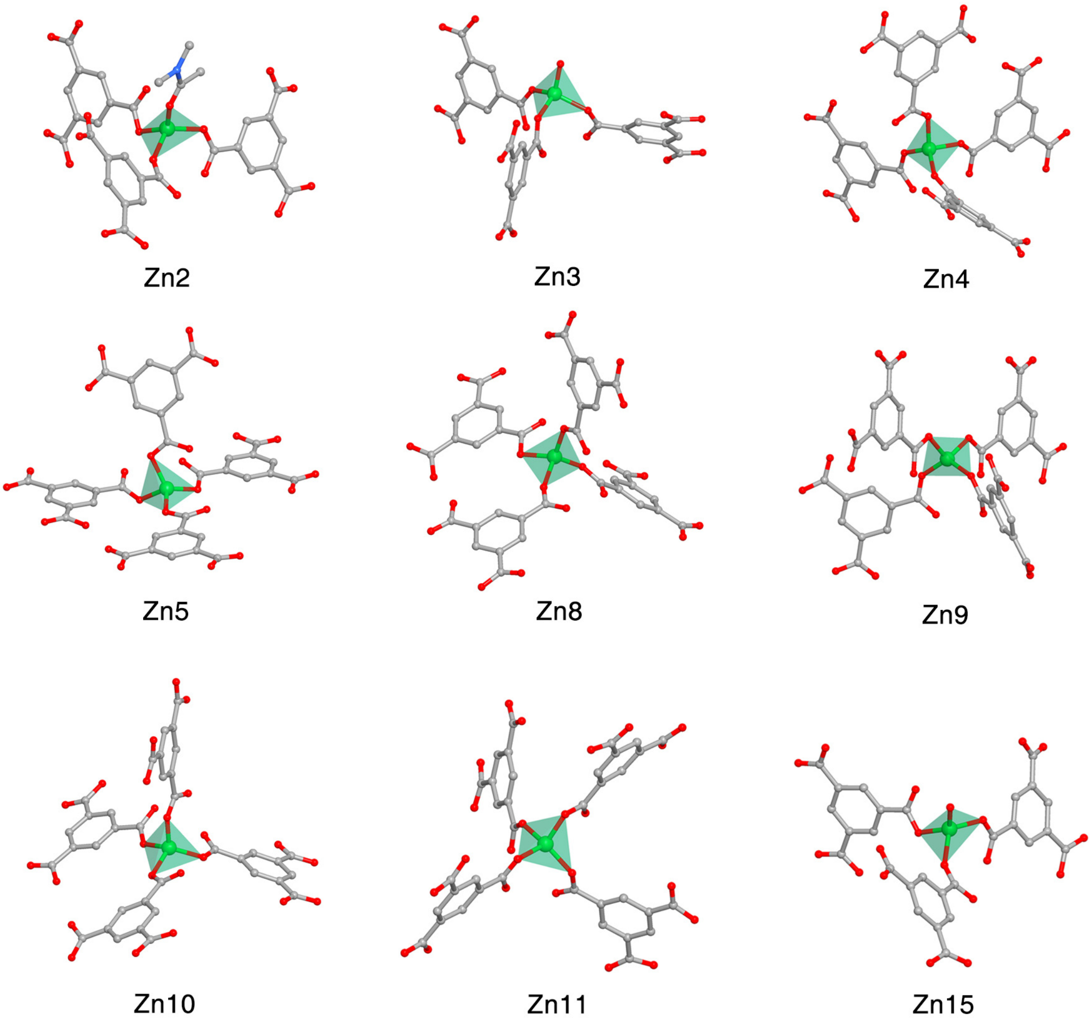

Figure S3 View of the nine tetrahedral Zn^{2+} ions of **1** and their coordination geometries with noticeable differences.

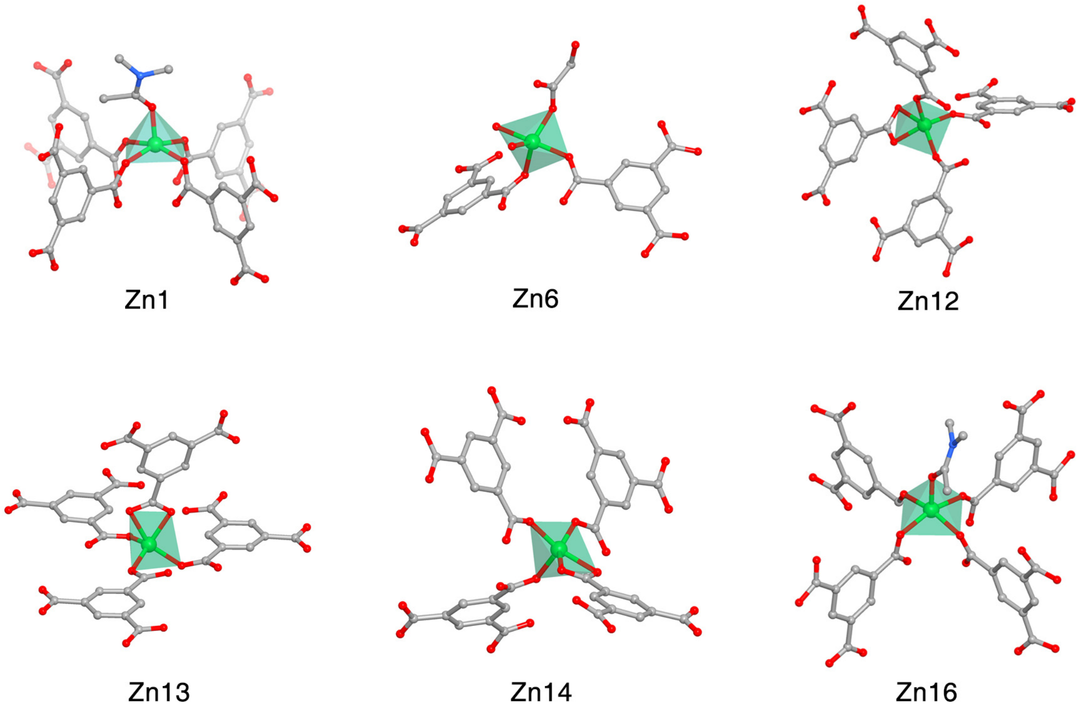

Zn1 Zn6 Zn12

Zn13 Zn14 Zn16

Figure S4 View of the six penta-coordinated Zn^{2+} ions of **1** and their coordination geometries with noticeable differences.

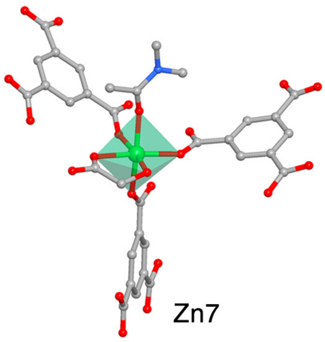

Figure S5 View of the octahedral Zn^{2+} ion and its coordination geometry.

(a) Four-metal-coordinated linkers

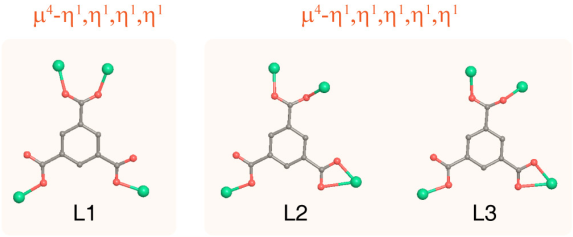

(b) Five-metal-coordinated linkers

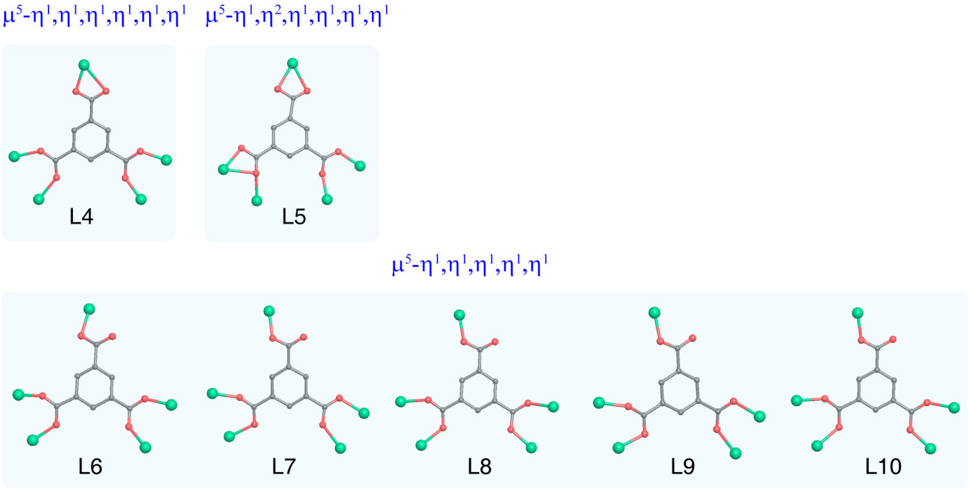

(c) Six-metal-coordinated linkers

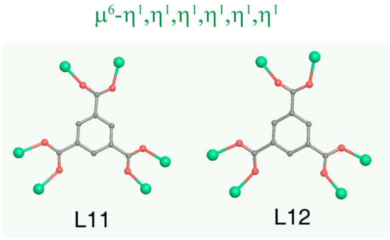

Figure S6 View of the coordination models of the twelve linkers in the asymmetric unit of **1**. The linkers are divided into three categories of (a) four-metal-coordinated with three linkers in two different models, (b) five-metal-coordinated with seven linkers in three different models, (c) six-metal-coordinated with two linkers.

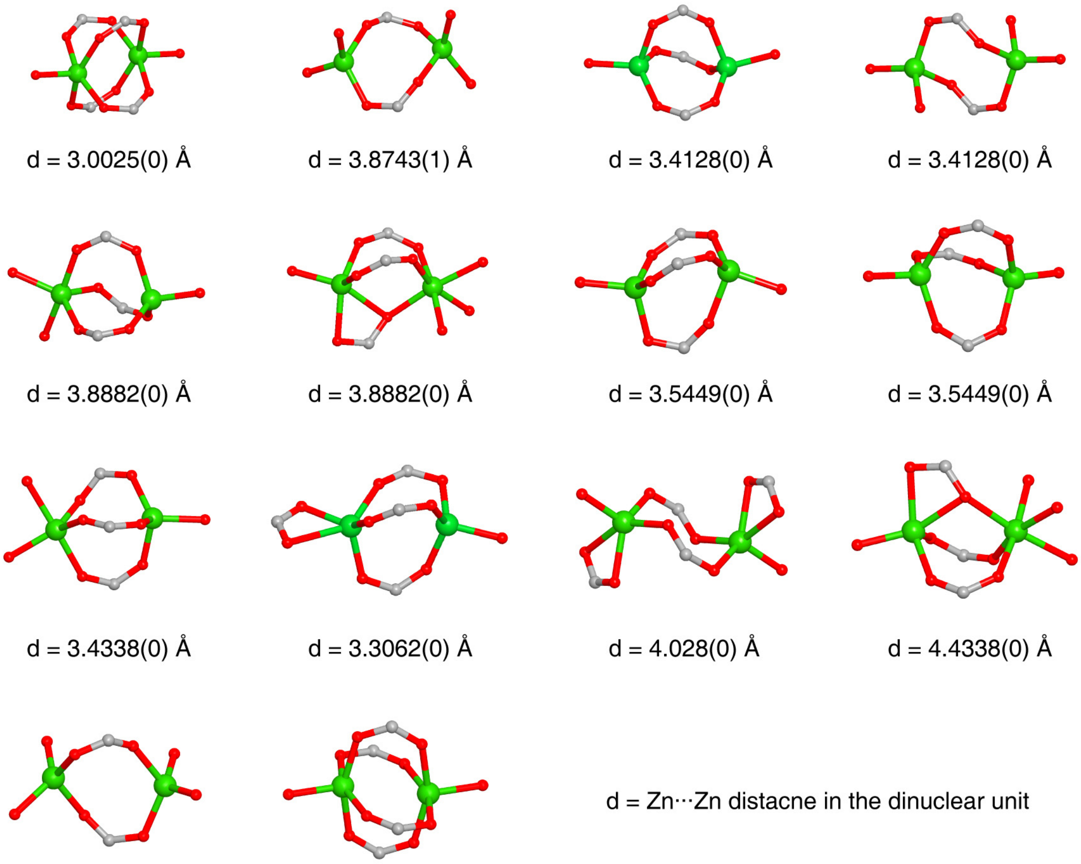

d = 3.0025(0) Å

d = 3.8743(1) Å

d = 3.4128(0) Å

d = 3.4128(0) Å

d = 3.8882(0) Å

d = 3.8882(0) Å

d = 3.5449(0) Å

d = 3.5449(0) Å

d = 3.4338(0) Å

d = 3.3062(0) Å

d = 4.028(0) Å

d = 4.4338(0) Å

d = 3.8743(0) Å

d = 2.8934(0) Å

d = Zn···Zn distacne in the dinuclear unit

Figure S7 Structural view of all the fourteen [Zn2] dinuclear units and the corresponding Zn···Zn distance in the dinuclear unit.

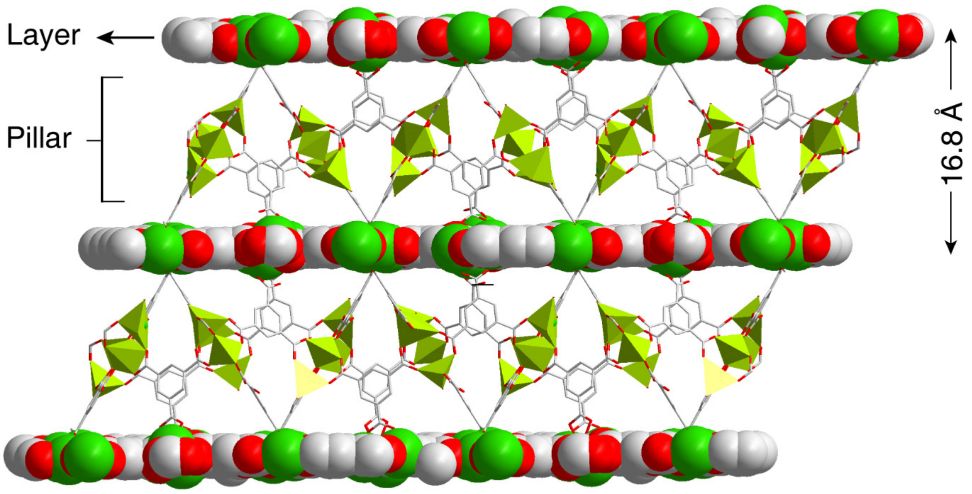

Figure S8 Perspective view of the pillared-layer structure of **1** with perpendicular distance of 16.8 Å bwtween adjacent layers. The layer are highlighted in space-filling modle, while the metal nodes in pillars are shown in polyhedron model for charity.

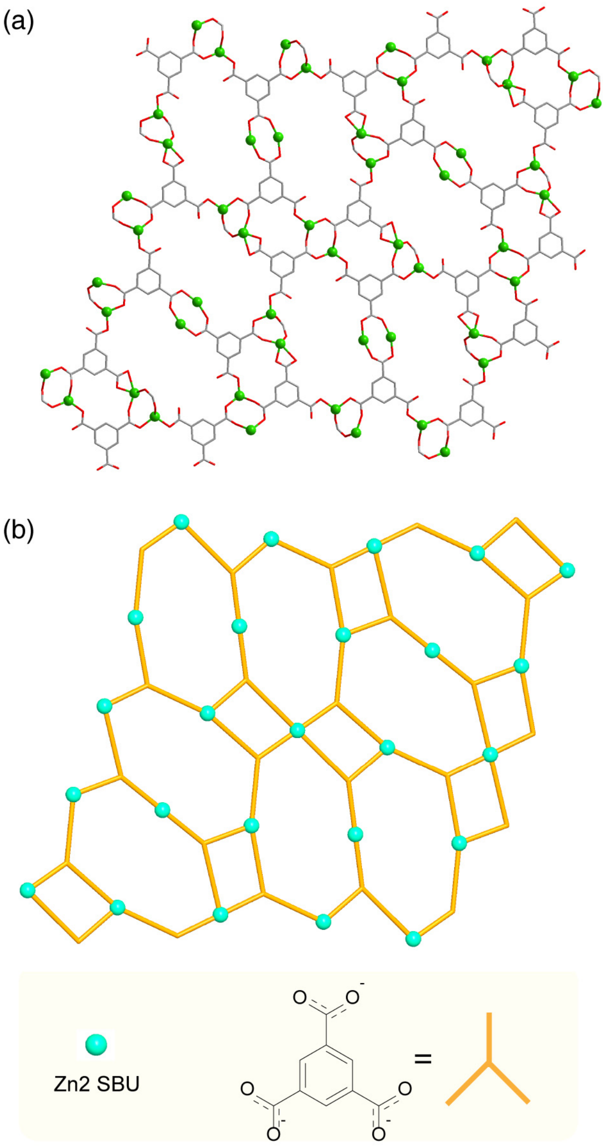

Figure S9 (a) Perspective view of the structure of layer in **1**, which are constructed from [Zn2] metal node and parallel-arranged linkers. (b) A simplified representation of the connectivity between the metal nodes and linkers within the layer.

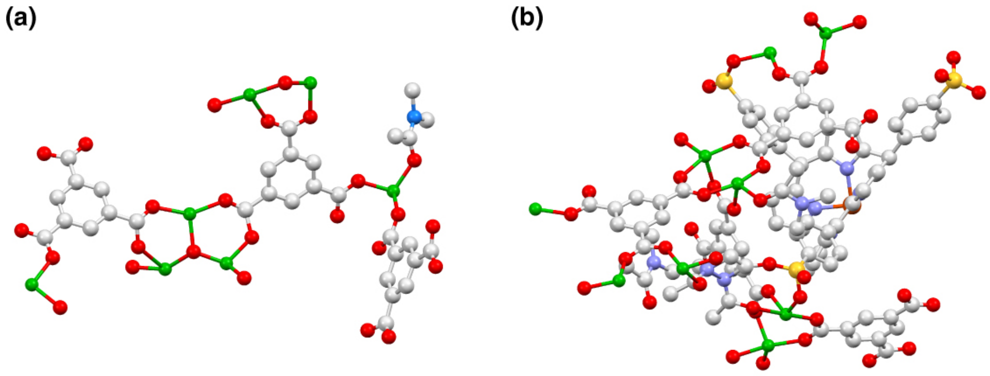

CCDC No. 916989

CCDC No. 1494844

Figure S10 View of the asymmetric unit of the reported Zn(II)-btc-MOFs with polynuclear composition containing (a) seven Zn^{2+} ions, and (b) nine Zn^{2+} ions.

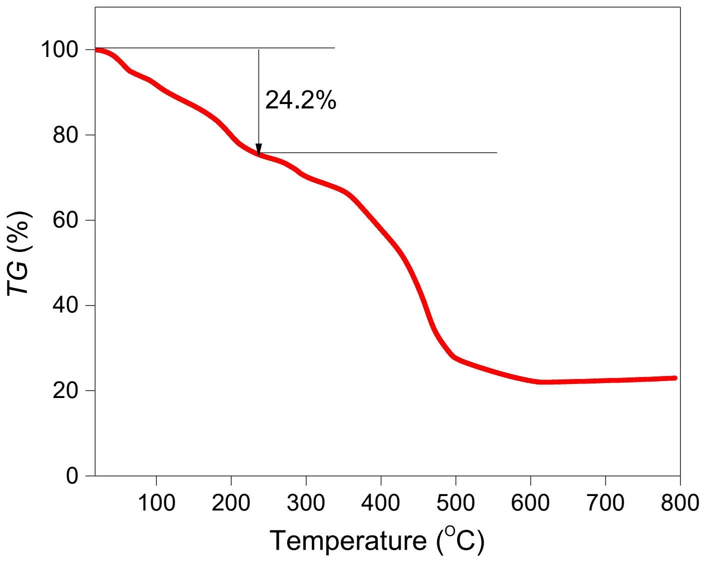

Figure S11 The thermogravimetric curves of **1** under N_2 atmosphere with a heating rate of 5 ºC/min in the temperature range of 30-800 ºC. The compound exhibits continuous weight loss without evident platform. There is a weigh loss of 24.2% before the spinodal at 230 ºC, which is attributed to the departure of guest DMA (Cal. 26.0%). Under further heating, continuous weight loss was observed, indicating the decomposition of the negative framework.

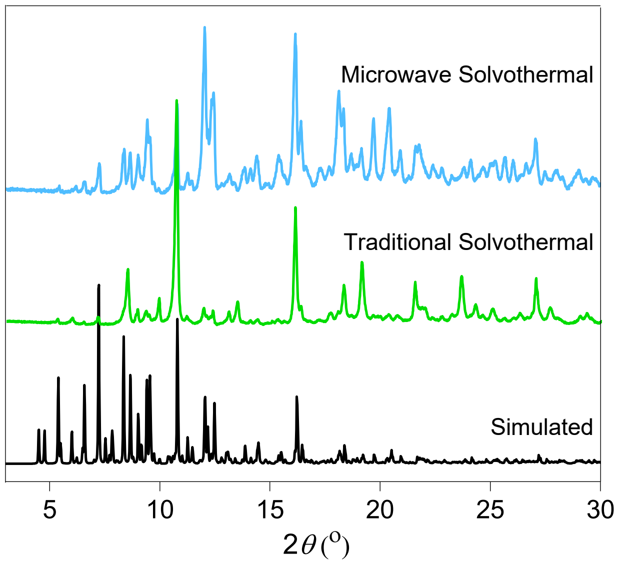

Figure S12 The PXRD patterns of **1** as simulated (black), synthesized by traditional solvothermal reaction (green), and synthesized by microwave-assisted solvothermal reaction (blue). The measured patterns are consistent to the simulated data with matched diffraction peaks, excepting the difference in intensity of each peak due to anisotropy of the crystals.

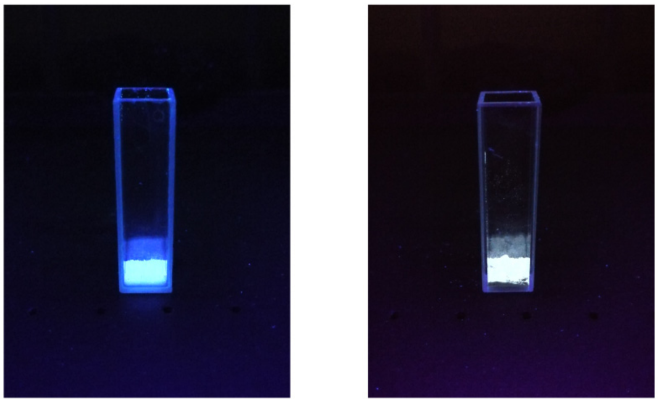

H_3btc (E_x = 365nm) 1 (E_x = 365nm)

Figure S13 The photograph of the solid state fluorescence of H_3btc and **1** under exication of 365 nm using a ultraviolet lamp.

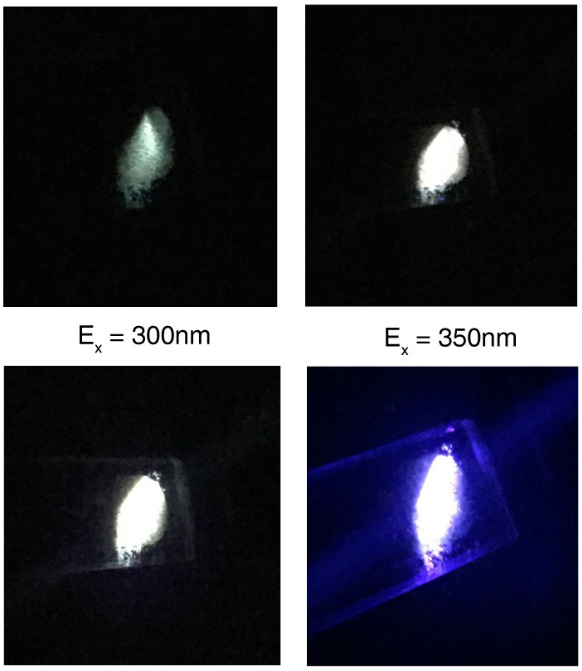

E_x = 300nm

E_x = 350nm

E_x = 400nm

E_x = 420nm

Figure S14 The photograph of the solid state fluorescence of **1** under different excitation of 300, 350, 400, and 420 nm, using the light from a fluorescence spectrophotometer. The crystals of **1** show white light emission under the wide range radiation of 300-400 nm.

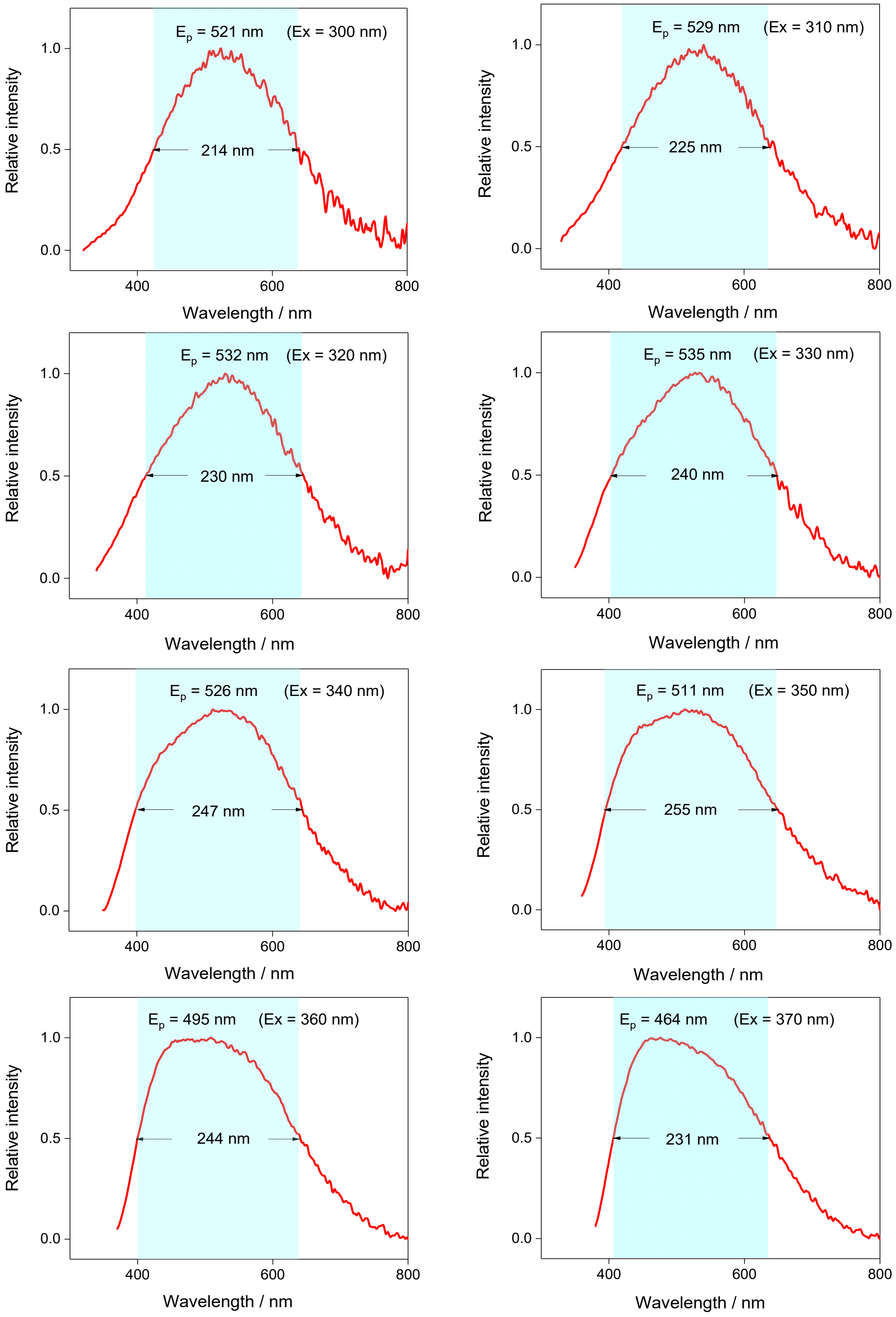
E_p = 521 nm (Ex = 300 nm)
214 nm
E_p = 529 nm (Ex = 310 nm)
225 nm
E_p = 532 nm (Ex = 320 nm)
230 nm
E_p = 535 nm (Ex = 330 nm)
240 nm
E_p = 526 nm (Ex = 340 nm)
247 nm
E_p = 511 nm (Ex = 350 nm)
255 nm
E_p = 495 nm (Ex = 360 nm)
244 nm
E_p = 464 nm (Ex = 370 nm)
231 nm
Relative intensity
0.0
0.5
1.0
Wavelength / nm
400
600
800

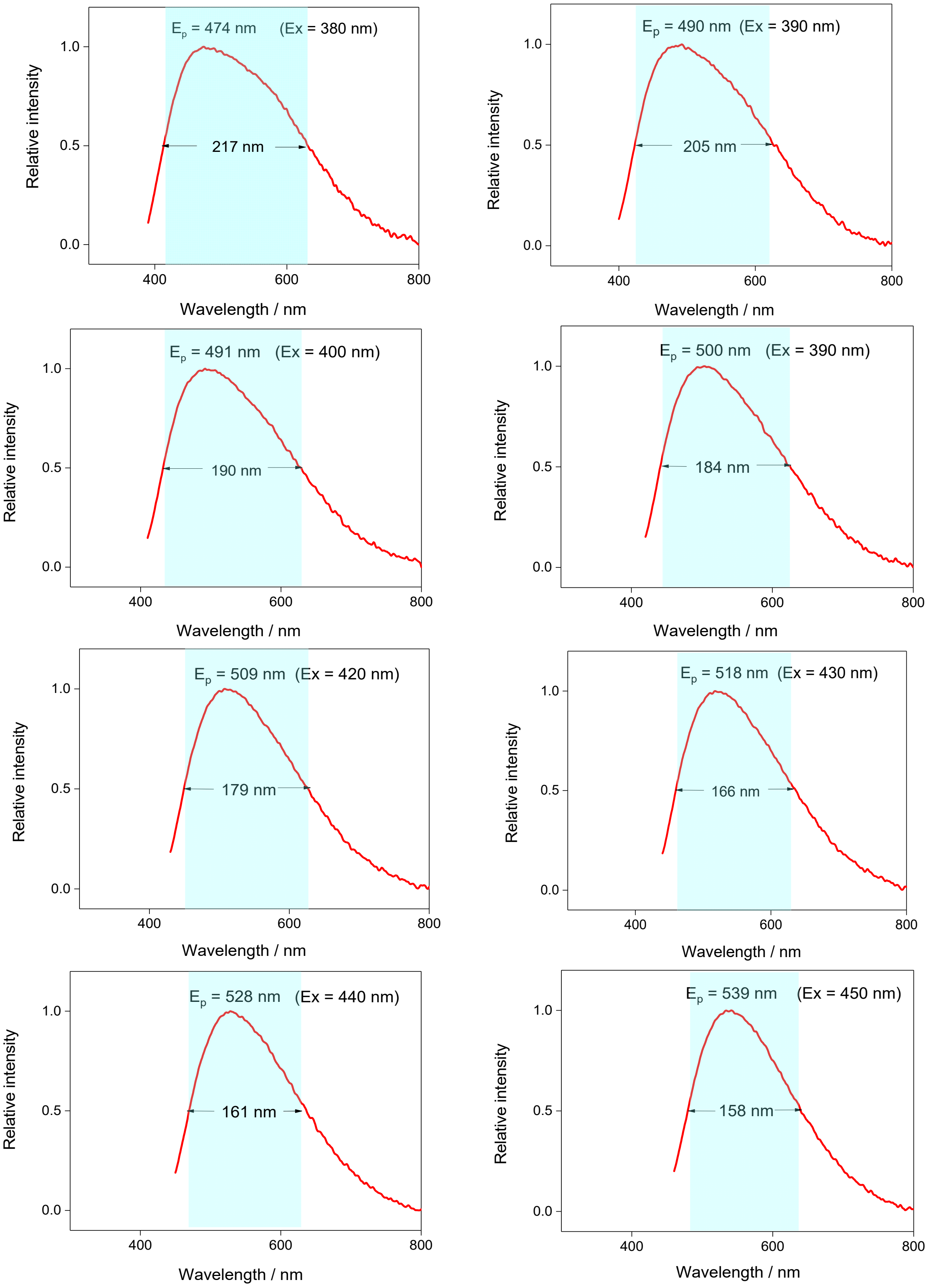

Figure S15 The fluorescence emission spectra with the peak position (E_P) of **1** under different excitation (E_X). The region of full width at half maxima of each spectra is highlighted in light blue.

Table S6 Statistics of the full width at half maxima (FWHM) for the emission spectra of **1** under different excitation from 300 to 380 nm.

E_x / nm	**E_p[a] / nm**	**E_{m1}[b] / nm**	**E_{m2}[c] / nm**	**FWHM / nm**
300	521	425	639	214
310	529	419	644	225
320	532	413	643	230
330	535	406	646	240
340	526	397	644	247
350	511	394	649	255
360	495	398	642	244
370	464	406	637	231
380	474	414	631	217

[a] Location of the emission spectrum with the maximum intensity. [b] The start point of emission spectrum with half maxima intensity. [c] The end point of emission spectrum with half maxima intensity.

Table S7 Statistics of the correlated color temperature (CCT) for the emission spectra of **1** under different excitation from 300 to 420 nm.

E_x / nm	CCT / K	E_x / nm	CCT / K
300	5749	370	6016
310	5750	380	6016
320	5750	390	5913
330	5765	400	5913
340	5810	410	5821
350	5885	420	5736
360	6020		

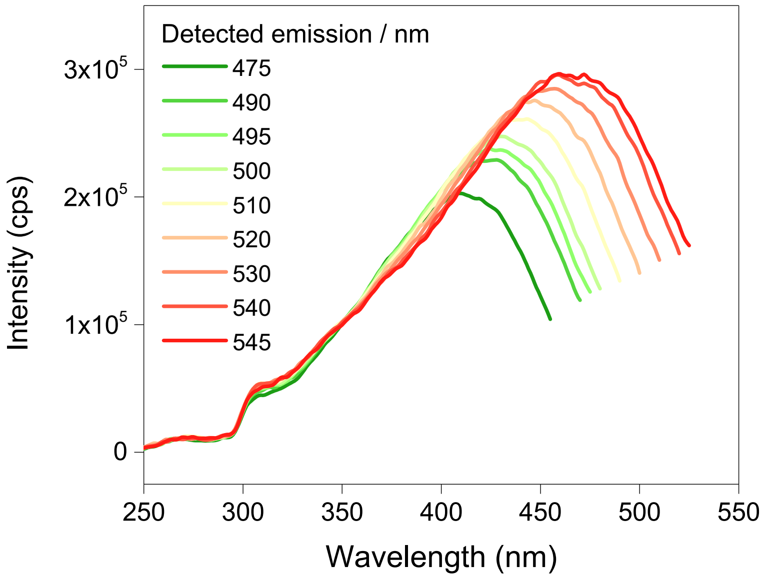

Figure S16 The fluorescence excitation spectra of **1** detected at different emission.

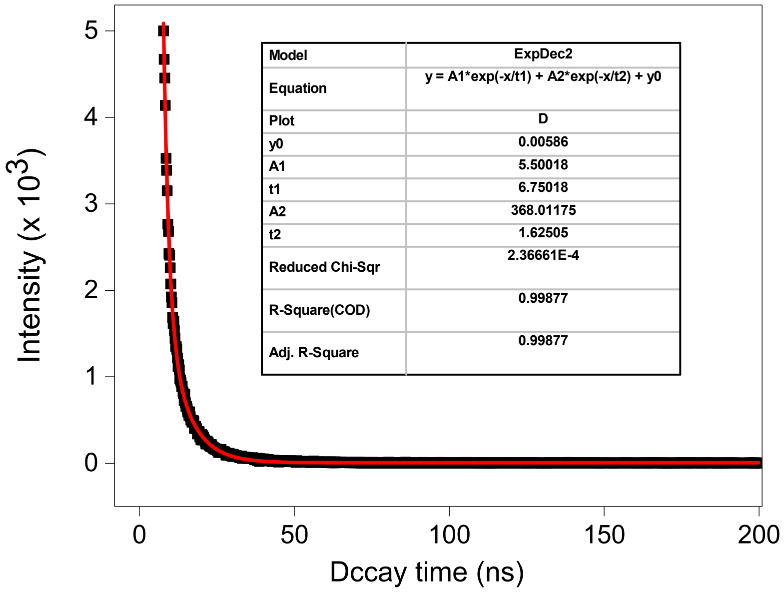

Model	ExpDec2
Equation	y = A1*exp(-x/t1) + A2*exp(-x/t2) + y0
Plot	D
y0	0.00586
A1	5.50018
t1	6.75018
A2	368.01175
t2	1.62505
Reduced Chi-Sqr	2.36661E-4
R-Square(COD)	0.99877
Adj. R-Square	0.99877

Figure S17 The decay time dependent emission intensity (black square) of **1**, giving the fitted (red line) fluorescence lifetime of 6.75 ns for **1**.

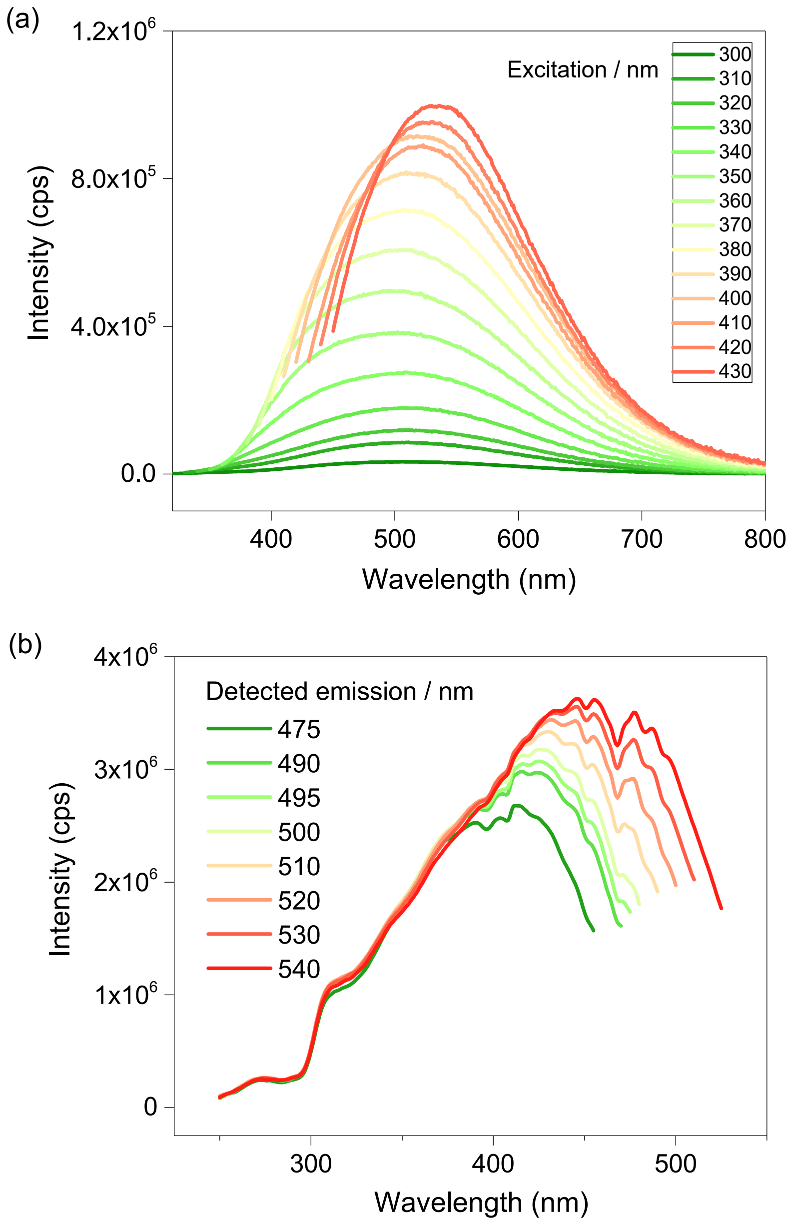

Figure S18 (a) The emission spectra of de-solvated **1** under different excitation. The as-synthesized MOFs were exchanged with dichloromethane and acetonitrile for more than 1 week until the original guest solvent of DMA was exchanged. The guest-exchanged samples were degassed at 323 K for 10 h to get the desolvated phase for fluorescence measurements. (b) The fluorescence excitation spectrum of de-solvated **1** detected at different emission.

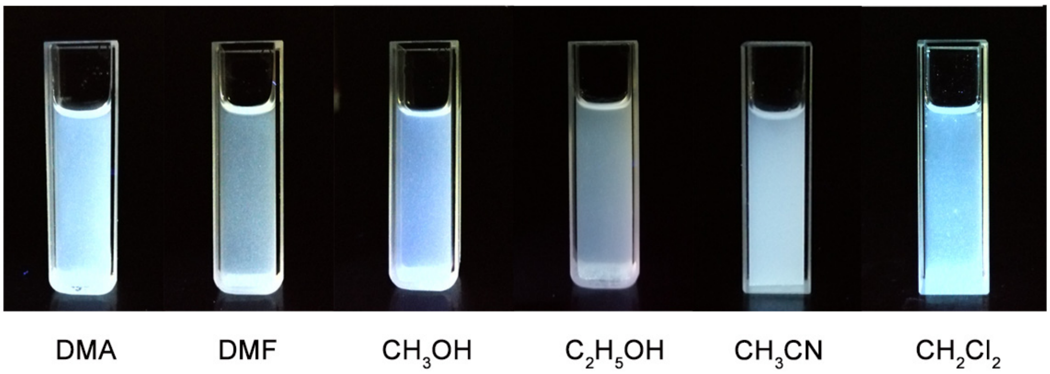

Figure S19 The photographs of the solution fluorescence of desolvated **1** in different organic solvents of DMA, DMF, CH_3OH, C_2H_5OH, CH_3CN and CH_2Cl_2, under excitation of 365 nm using a ultraviolet lamp. The suspensions were prepared by dispersing 5 mg fine-ground crystals of desolvated **1** into 3 mL solvent, followed by ultrasonic treatment for 20 minutes.

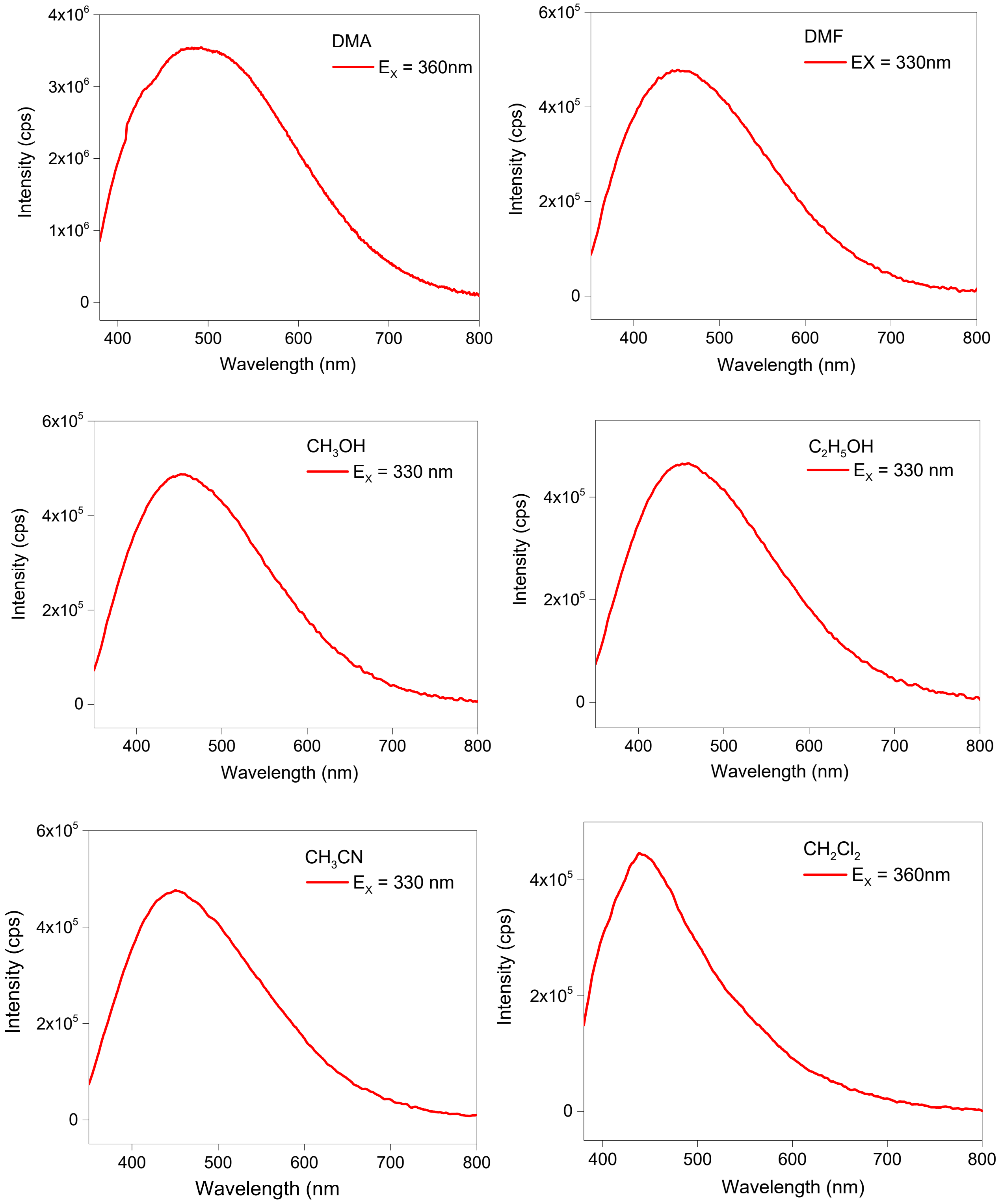

Figure S20 The emission spectra for suspension of desolvated **1** in DMA, DMF, CH_3OH, C_2H_5OH, CH_3CN, and CH_2Cl_2, which exhibits continuous and broadband spectra.

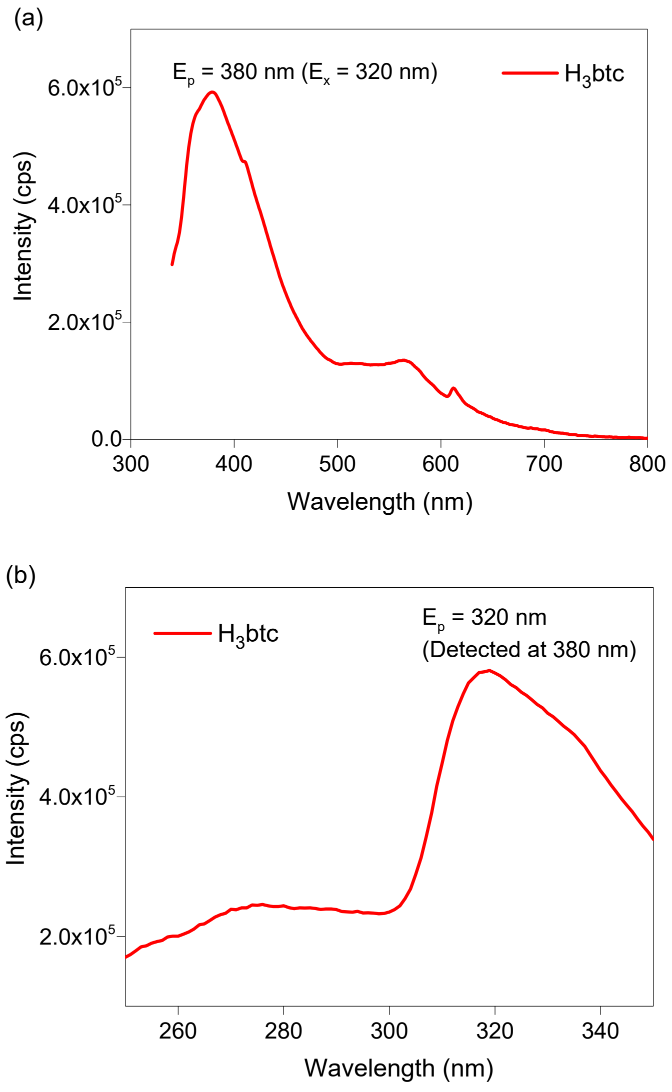

Figure S21 The (a) emission and (b) excitation spectra of the free ligand H_3btc.

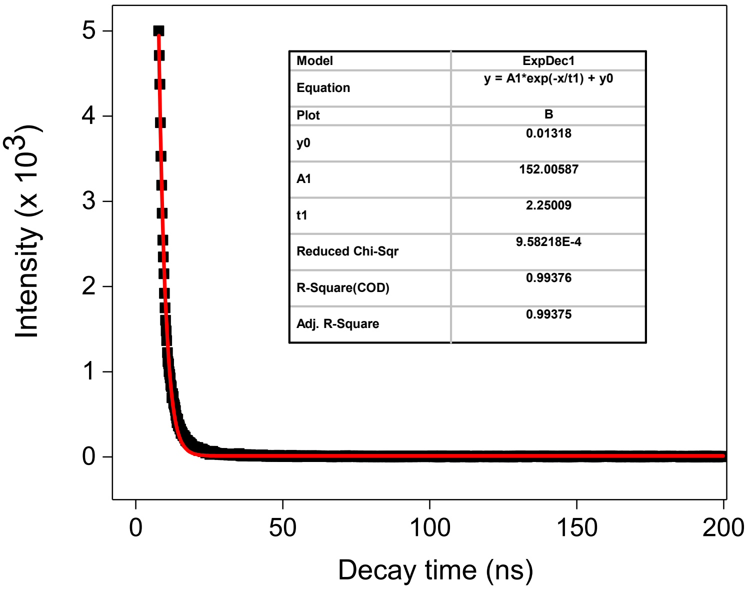

Figure S22 The decay time dependent emission intensity (black square) of the free ligand of H_3btc, giving the fitted (red line) fluorescence lifetime of 2.25 ns for H_3btc.

Refference:

1. G. M. Sheldrick, *Acta Crystallogr. A*, 2008, **64**, 112.

2. O. V. Dolomanov, L. J. Bourhis, R. J. Gildea, J. A. K. Howard and H. Puschmann, *J. Appl. Cryst.*, 2009, **42**, 339.

3. A. L. Spek, *J. Appl. Crystallogr.*, 2003, **36**, 7.

4. A. L. Spek, *Acta Cryst.* 2015, **C71**, 9.

5. X.-R. Hao, X.-L. Wang, K.-Z. Shao, G.-S. Yang, Z.-M. Su and G. Yuan, *CrystEngComm*, 2012, *14*, 5596.